TS-Fuzzy Associated DTC of Three Phase Induction Motor Drive for Water Pumping from Single Phase Supply

Ramakrishna Raghutu, Vasupalli Manoj and Narendra Kumar Yegireddy

Dr. Ramakrishna Raghutu, Assistant Professor, Department of Electrical and Electronics Engineering, GMR Institute of Technology, Rajam, Vizianagaram, Andhra Pradesh, India – 532127.
Dr. Vasupalli Manoj, Assistant Professor, Department of Electrical and Electronics Engineering, GMR Institute of Technology, Rajam, Vizianagaram, Andhra Pradesh, India – 532127.
Dr. Narendra Kumar Yegireddy, Professor, Department of EEE, Satya Institute of Technology and Management, Vizianagaram, Andhra Pradesh, India – 535003.

Abstract: Aqua farms necessitate an uninterrupted power supply in order to run three-phase induction motors and sustain optimal oxygen levels. Hence, it is necessary to convert single to three-phase power in order to operate the motors and use diesel generators during power outages. Unfortunately, heavy diesel consumption poses challenges in aqua culture. To address this, integrating a photovoltaic (PV) and wind generator system can help reduce diesel consumption. However, both wind and solar energy are dependent on nature and unpredictable. Therefore, a small-sized battery is also integrated into the system. An effective energy management system is essential for achieving a cost-efficient system with optimal performance. The battery is employed to respond during transitional time periods. The suggested energy management system has the capability to minimize diesel usage by operating at peak efficiency. The battery can be replenished from both PV and wind sources. Any surplus power from these sources can be transferred to the single-phase grid in order to decrease electricity expenses. DC to DC converters, based on sliding mode controllers, are integrated to uphold a steady DC-link voltage. The supply from the single-phase grid is converted to DC and then boosted to the rated voltage to obtain sufficient three-phase AC voltage through an inverter. The proposed controller aims to reduce ripples in motor torque, thereby improving the lifetime of system components and reducing power consumption. An induction motor is controlled using a TS-Fuzzy based speed sensorless direct torque controller and a three-phase inverter to reduce torque fluctuations. The performance of the proposed system is validated using the Hardware – in the – Loop (HIL) on OPAL-RT platform associated with MATLAB/Simulink, and the results are presented comprehensively to demonstrate its effectiveness in both steady state and transient conditions.

Corresponding Author: ramakrishna.r@gmrit.edu.in

Keywords: Water pumping system, Induction motor, Sliding mode controller,
Direct torque controller, TS-Fuzzy, PV, Wind, Renewable Energy Sources.

Acknowledgement:
The authors would like to thank the management of GMR Institute of Technology, Rajam, Vizianagaram for the constant support and encouragement rendered by them and also for providing us various facilities including OPAL-RT devices to achieve the outcome of this research paper.

1. Introduction

Water is a vital resource for human survival and plays a crucial role in the progress of nations. Given the scarcity of water resources close to human settlements, the extraction of water from underground sources has become imperative. Consequently, water pumping systems have become an essential component of human existence, catering to both agricultural and drinking needs. Moreover, a reliable water supply is indispensable for the efficient functioning of aqua farms. To achieve this, an induction motor is linked with a water pump. In certain instances, motors are also necessary to maintain oxygen levels in aquaculture. An electric motor is essential for driving the pump. However, when lifting substantial amounts of water from deep underground, high power and torque motors are essential. Consequently, due to the limited availability of single-phase electrical supply in many areas, it becomes necessary to convert the single-phase supply to DC using a diode rectifier in order to operate an induction motor supplied by three phase. Nevertheless, the DC voltage produced might not meet the requirements to operate the three-phase motor using an inverter. To overcome this, a boost converter is required to increase the voltage. Nevertheless, the pulsating DC output voltage of the diode rectifier is not suitable for the operation of the inverter. In order to resolve this concern and maintain a steady DC output from the boost converter, it is essential to incorporate a Sliding Mode Controller (SMC). The SMC guarantees a reduction in harmonics by stabilizing the DC output, which in turn results in a smoother input voltage for the inverter. Therefore, water pumping systems are best suited with three-phase motors. This leads to an enhanced motor lifespan compared to high harmonics.

Researchers have suggested the utilization of induction motors for water pumping systems, a practice already prevalent in India. Hence, this study has opted for an induction motor for the enhancement of a water pumping system. Typically, submersible pumps are employed in such systems, necessitating the motor to be submerged at a considerable depth underground. This setup can present challenges in accurately monitoring the motor's speed. To tackle this issue, a speed sensorless controller has been integrated into this study. Moreover, to reduce torque fluctuations, the motor is operated using a Direct Torque Controller (DTC) via an inverter. Additionally, Takagi-Sugeno (TS) fuzzy-based controllers are combined with DTC to produce a reference electromagnetic torque.

Power outages are a common occurrence in various locations, including aqua farms. As a result, farmers often rely on diesel engines or generators to ensure uninterrupted operation of their motors. However, the use of diesel generators not only consumes a significant amount of diesel fuel but also releases toxic gases that can harm aquatic life. To address this issue and reduce diesel consumption, renewable energy sources have been incorporated into the system. Presently, photovoltaic and wind energies are widely recognized and utilized. Therefore, PV and DC generator-based wind power generation systems have been integrated to provide power to the motors when there is no supply from the grid. However, it is crucial to acknowledge that the production from PV and wind sources is not consistent. To overcome this challenge, a battery bank has been incorporated into the system.

2. System Overview

Figure 1 depicts the proposed water pumping system, which employs a 3-ph induction motor powered by a single-phase source. The setup comprises different elements, including a single-phase diode rectifier for transforming the single-phase input into DC, along with a boost converter for increasing the DC voltage to maintain a steady DC-link voltage. Subsequently, this voltage is fed into an inverter, which transforms it into AC supply for the three-phase motor. The induction motor is responsible for propelling the water pump.

To maintain stability in the DC-link voltage, a SMC is employed to generate pulses for Q_1. In comparison to the PI, the TS-Fuzzy controller offers an advantage in reducing torque ripples by deriving the reference motor torque. The TS-Fuzzy controller ensures a smooth output through its simple defuzzification rules. The DTC method is utilized for speed regulation of the motor, allowing for adjustment of the discharged water amount from the pump. Furthermore, the utilization of space vector pulse width modulation is employed to generate pulses for the inverter. To summarize, the elements depicted in Figure 1 have been succinctly described.

The MPPT converters are employed to enhance the individual performances of the PV and wind generators. The DC generator is responsible for generating a direct current power source. The battery is connected to the DC bus through a bidirectional circuit. The bidirectional circuit regulates the voltage of the DC bus by controlling whether to charge or discharge the battery based on the power availability from the PV and wind sources. The excess electricity produced by the renewable energy sources is transmitted to the power grid through a converter that can transfer power in both directions, operating on a single-phase system. However, the battery cannot be charged from the grid due to this issue, prompting the addition of a diode between the DC bus and the single-phase bidirectional converter.

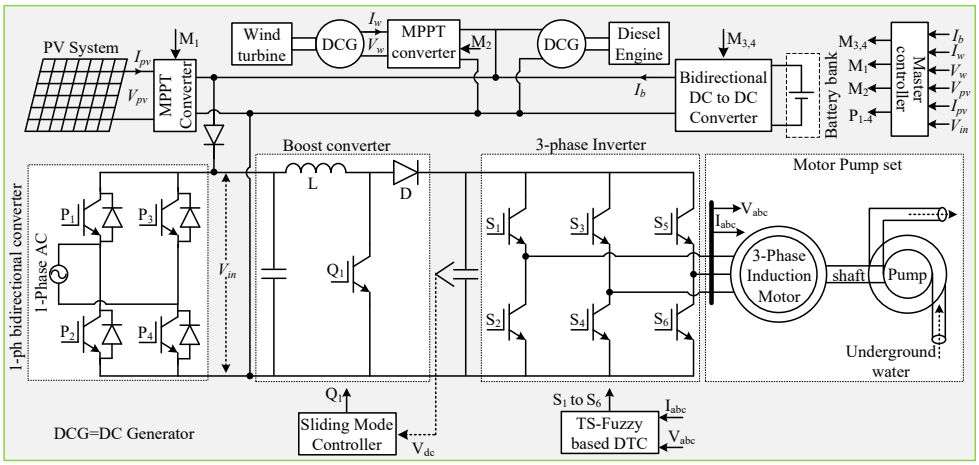

Fig. 1: Proposed model with 3 phase induction motor.

A. Selection of motor ratings and pump

The water pump necessitated a certain amount of force in order to raise the water, a force that could be generated by a motor. Typically, the motor/pump should have a minimum torque known as the breakaway torque (T_b), which should be approximately 10 to 25% of the torque required to overcome the static friction and lift the water from underground. The

motor must surpass the base value (ωt) of its speed in order for the pump to initiate the delivery of water. The flow rate of water (Q, gal/min) is directly proportional to the speed of the pump/motor (ω), as indicated in equation (1) derived from curve fitting [25]. Furthermore, the system's leader is controlled by a non-linear equation denoted as equation (2).

$$Q = \begin{cases} a\omega - b & \omega \geq \omega_t \\ 0 & \omega < \omega_t \end{cases} \quad (1)$$

$$H = a_0\omega^2 + a_1\omega Q + a_2 Q^2 \quad (2)$$

And,

$$W_{hp} = \frac{Q \times H}{3960} \quad (3)$$

Where, a, a_0, a_1, a_2 and b are constants. W_{hp} = required horse power. H is total dynamic head. The brake horse power (*BHP*) of the motor given by.

$$BHP = W_{hp} / (\text{Drive efficiency} \times \text{Pump efficiency}) \quad (4)$$

Given that Q_{max} is 100 gallons per minute, H is 50 meters, and the pump efficiency is 1, with a drive efficiency of 0.95, equation (4) indicates that approximately 5 horsepower is needed to lift the necessary water. Equation (2) further reveals that the maximum speed of the motor is 190 radians per second, which is approximately equal to 1800 revolutions per minute.

The motor's torque, denoted as TL, is equal to 25 Nm. However, as water is being pumped from underground to ground level, the load torque will gradually increase from Tb to TL due to the increasing weight of the water on the motor. At first, the load torque will start off low and increase steadily in a ramp-like manner as the water is released to ground level. Upon reaching ground level, the water will maintain a constant load torque. Additionally, the friction between the pipe and the water will introduce an additional load torque on the motor. Furthermore, if extra pipes are added to supply water to other locations, the load torque will increase accordingly. Typically, a 5 hp motor is used in the agricultural sector to supply water for crops. Similarly, a 5 hp motor is employed in the aquaculture sector to circulate oxygen in ponds. However, for apartment buildings with five floors, a 3 hp motor is sufficient to lift water and store it in water tanks.

B. Boost converter with SMC

In order to run a three-phase induction motor with a single-phase power source, a three-phase inverter is utilized to transform the power into DC. Nevertheless, the diode rectifier produces an oscillating DC voltage that requires smoothing to reduce the ripple factor of the induction motor. In order to accomplish this, a SMC (Switched Mode Converter) is utilized to implement a boost converter that provides a steady DC output supply. Figure 2 illustrates the implemented SMC, which generates pulses for Q_1.

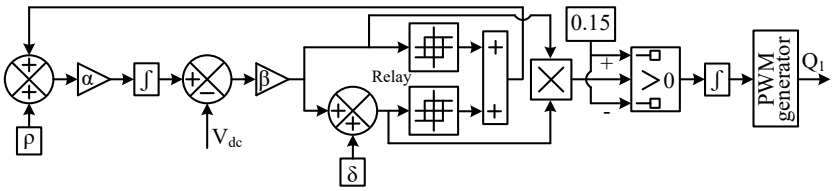

Fig. 2: Sliding mode controller for boost converter.

C. Sensorless control of induction motor

Most water pumping systems typically consist of submersible pumps, with the motor also submerged underwater. To effectively design a speed control system for the induction motor, it is crucial to sense the motor's speed. However, this becomes challenging when the motor is submerged at great depths. Therefore, the estimation of speed through mathematical equations can be utilized to develop a sensorless speed controller for the induction motor.

Various control methods, including v/f control, indirect field-oriented control (IFOC), vector control, and slip control, can serve as the basis for IM drive [2, 28-36]. Among these, IFOC and slip control are particularly effective in decoupling the controls of flux and torque. IFOC, in particular, is a simple and suitable option for water pumping systems [2, 12-13]. This document utilizes sensorless vector control, considering the benefits of sensorless control in submersible water pumping systems. Figure 3 depicts the speed estimation process for the IM using a model reference adaptive controller (MRAC), as shown in the block diagram. Accurate speed estimation is of utmost importance in sensorless speed control, and it can be achieved by utilizing mathematical expressions [28, 34-36]. Nevertheless, in order to carry out this estimation procedure, it is essential to have access to the input voltage and currents of the IM. This, in turn, requires the utilization of voltage and current sensors. Fortunately, the positive aspect is that a mere two current sensors are adequate for sensing the current of 3-phs, while the input voltages can be acquired through phase voltage reconstruction, as depicted in Figure 3. The inverter's output, which acts as the IM's input, relies on both V_{dc} and the pulses generated by the PWM generator. Consequently, the inverter voltages can be determined using mathematical expressions [36]. As a result, there is no need for physical voltage sensors to detect the input voltage of the IM, leading to a system that is more economical.

The speed can be estimated by the following equations [28, 34-36]:

$$v_{ds}^{s} = i_{ds}^{s} R_s + L_{ls} \frac{d}{dt}\left(i_{ds}^{s}\right) + \frac{d}{dt}\left(\psi_{dm}^{s}\right) \tag{5}$$

$$v_{ds}^{s} = \frac{L_m}{L_r} \frac{d}{dt}\left(\psi_{dr}^{s}\right) + \left(R_s + \sigma L_s S\right) i_{ds}^{s} \tag{6}$$

where, $\sigma = 1 - \frac{L_m^2}{L_r L_s}$

$$\frac{d}{dt}\left(\psi_{dr}^{s}\right) = \frac{L_r}{L_m} v_{ds}^{s} - \frac{L_r}{L_m}\left(R_s + \sigma L_s S\right) i_{ds}^{s} \tag{7}$$

Similarly

$$\frac{d}{dt}\left(\psi_{qr}^{s}\right) = \frac{L_r}{L_m} v_{qs}^{s} - \frac{L_r}{L_m}\left(R_s + \sigma L_s S\right) i_{qs}^{s} \tag{8}$$

$$\frac{d}{dt}\left(\psi_{dr}^{s}\right) = \frac{L_m}{T_r} i_{ds}^{s} - \omega_r \psi_{qr}^{s} - \frac{1}{T_r} \psi_{dr}^{s} \tag{9}$$

$$\frac{d}{dt}\left(\psi_{qr}^{s}\right) = \frac{L_m}{T_r} i_{qs}^{s} + \omega_r \psi_{dr}^{s} - \frac{1}{T_r} \psi_{qr}^{s} \tag{10}$$

where, $T_r = \frac{L_r}{R_r}$

Moreover, rotor angle is:

$$\theta_e = \tan^{-1}\left(\frac{\psi_{qr}^s}{\psi_{dr}^s}\right) \tag{11}$$

Hence, rotor speed is calculated by below equation,

$$\omega_r = \frac{d}{dt}\theta_e = \frac{1}{\psi_r^2}\left[\left(\psi_{dr}^s \frac{d}{dt}\psi_{qr}^s - \psi_{qr}^s \frac{d}{dt}\psi_{dr}^s\right) - \frac{L_m}{T_r}\left(\psi_{dr}^s i_{qs}^s - \psi_{qr}^s i_{ds}^s\right)\right] \tag{12}$$

Slip speed is:

$$\omega_{slip} = \frac{(1+\sigma T_r S)L_s i_{qs}}{T_r(\psi_{ds} - \sigma L_s i_{ds})} \tag{13}$$

Hence, the speed of IM is:

$$\omega = \omega_{slip} + \omega_r \tag{14}$$

The complete block diagram of speed estimation with the help of equation from (5) to (14) is shown in Fig. 3.

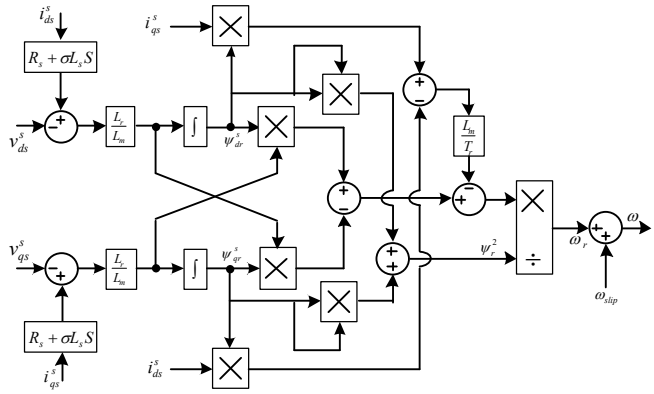

Fig. 3: Speed estimation by MRAC

D. TS-Fuzzy controller

Typically, the TS-Fuzzy controller demonstrates superior performance in handling abrupt changes in the dc-link voltage compared to the Proportional+Integral (PI) controller [4]. Below, you will find a comprehensive explanation of the implementation of the TS-Fuzzy controller.

The input variables for the designed TS-Fuzzy are the error variations of voltage/current (xi) and its derivative (xi') signals, as depicted in Figure 4. To fuzzify the inputs, two membership functions (MFs) are used: positive (P) and negative (N), as shown in Figure 4. The MFs for the xi and xi' signals are defined in equations (15) and (16) respectively. The corresponding rules for the TS-Fuzzy controller can be found in Table 5.

$$\mu_{\mathrm{P}}(x_{\mathrm{i}})=\begin{cases}0, & x_{\mathrm{i}}<L_1\\ \dfrac{x_{\mathrm{i}}+L_1}{2L_1}, & -L_1\le x_i\le L_1 \text{ and}\\ 1, & x_{\mathrm{i}}>L_1\end{cases}$$

$$\mu_{\mathrm{N}}(x_{\mathrm{i}})=\begin{cases}1, & x_{\mathrm{i}}<L_1\\ \dfrac{-x_{\mathrm{i}}+L_1}{2L_1}, & -L_1\le x_{\mathrm{i}}\le L_1\\ 0, & x_{\mathrm{i}}>L_1\end{cases} \quad (15)$$

$$\mu_{\mathrm{P}}(\dot{x}_{\mathrm{i}})=\begin{cases}0, & \dot{x}_{\mathrm{i}}<L_2\\ \dfrac{\dot{x}_{\mathrm{i}}+L_2}{2L_2}, & -L_2\le \dot{x}_{\mathrm{i}}\le L_2 \text{ and}\\ 1, & \dot{x}_{\mathrm{i}}>L_2\end{cases}$$

$$\mu_{\mathrm{N}}(\dot{x}_{\mathrm{i}})=\begin{cases}1, & \dot{x}_{\mathrm{i}}<L_2\\ \dfrac{-\dot{x}_{\mathrm{i}}+L_2}{2L_2}, & -L_2\le \dot{x}_{\mathrm{i}}\le L_2\\ 0, & \dot{x}_{\mathrm{i}}>L_2\end{cases} \quad (16)$$

Table 1 presents the calculated output of the TS-Fuzzy operation, where $Z_{1\text{-}4}$, characterize the results. The sampling instant is denoted by K. The fuzzy constants, $a_{1\text{-}5}$, are designated and adjusted through a tuning process specific to each controller. To obtain the controller's output (Y), a generalized defuzzifier is utilized, as described in equation (17).

$$Y=\frac{Z_1K_1+Z_2K_2+Z_3K_3+Z_4K_4}{Z_1+Z_2+Z_3+Z_4} \quad (17)$$

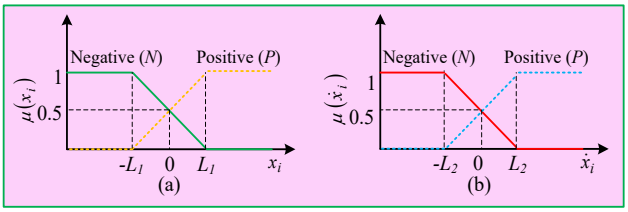

Fig. 4: TS-Fuzzy MFs.

Table 1: Rules of a TS-fuzzy controller:

Rule	x_i(k)	$\dot{x}_i$(k)	Value
RuleA	*N*	*N*	$Z_1=\mathrm{a}_1x_i(\mathrm{i})+\mathrm{a}_2\dot{x}_i(\mathrm{i})$
RuleB	*N*	*P*	$Z_2=Z_1\mathrm{a}_3$
RuleC	*P*	*N*	$Z_3=Z_1\mathrm{a}_4$
RuleD	*P*	*P*	$Z_4=Z_1\mathrm{a}_5$

It should be noted that the output Y undergoes dynamic adjustments through the application of TS-Fuzzy, resulting in enhanced stability and performance, especially during rapid dynamical system events.

The proposed system utilizes TS-Fuzzy to create a reference torque through the comparison of the motor's speed with its reference speed. As a result, the effective application of a

seamless reference torque signal can greatly reduce the fluctuations in the electromagnetic torque produced by the induction motor.

3. Proposed DTC with TS-Fuzzy

The DTC is a sophisticated method employed in variable frequency drives, particularly for Induction Motors. It involves analyzing the measured voltage and current of the motor to estimate its magnetic flux and torque. The DTC of the induction motor exhibits the subsequent attributes:

- By modifying the reference signals for torque and flux, the motor can promptly track its desired values with the generated actual values.
- TThere will be no occurrence of a step response with peak overshoot.
- The necessary computations are performed within a fixed reference frame.
- The switch control signals are directly defined by the hysteresis control, eliminating the need for a separate modulator.
- The tuning of PI controllers is unnecessary for controlling torque directions. Therefore, there is no requirement for tuning.
- The switching frequency varies, ensuring minimal current and torque ripple.
- As a result of the hysteresis control implemented in the switching process, the current spectrum remains free from any peaks. Consequently, the machine produces minimal audible noise.
- The algorithm automatically considers the voltage variation in the intermediate DC circuit, specifically in voltage integration. As a result, there are no issues arising from DC voltage ripple or DC voltage transients.
- Synchronizing with a rotating machine is a simple process thanks to the rapid control mechanism. Adjust the torque reference to zero before starting up the inverter. The flux will be determined by the initial current pulse.
- Digital control equipment must possess high speed capabilities to effectively maintain the flux and torque within the specified tolerance limits. Generally, the control algorithm needs to be executed at intervals of 10 - 30 microseconds or even shorter. Despite this rapid execution, the algorithm itself is relatively simple, resulting in a minimal number of calculations.
- To ensure effective hysteresis control, it is imperative to utilize high-quality current and voltage measuring devices that are free from noise and equipped with low-pass filtering capabilities. The presence of noise and slow response in these devices can significantly impair the accuracy and efficiency of hysteresis control.
- At higher velocities, the method remains unaffected by any motor parameters. Nevertheless, when operating at lower speeds, the accuracy of stator flux estimation is significantly impacted by the error in stator resistance.

The DTC method demonstrates excellent performance under various conditions, even without the need for speed sensors. Nevertheless, the estimation of flux typically relies on integrating the motor phase voltages. As a result, achieving motor control becomes impossible when the output frequency of the variable frequency drive drops to zero. Additionally, the motor can also rotate in the reverse direction at any given moment.

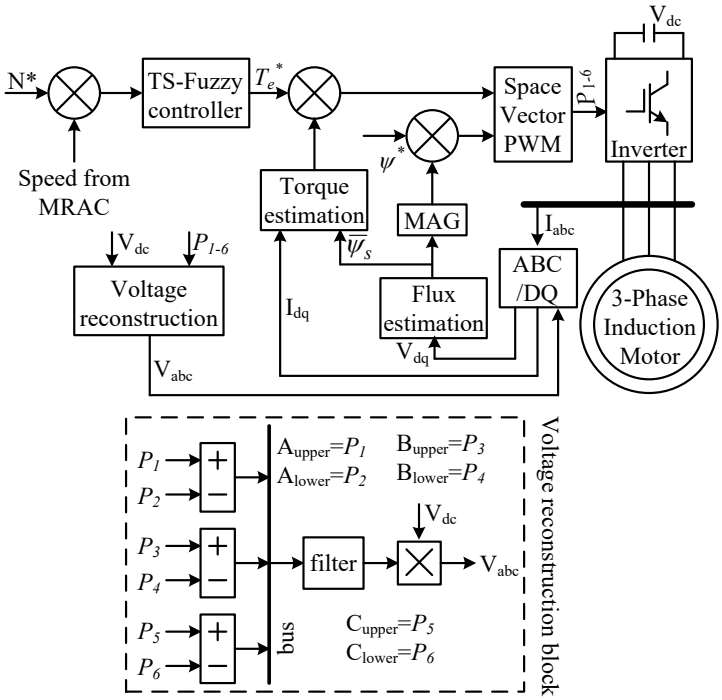

Fig. 5: Proposed control of IM.

The DTC technique effectively selects one of the six non-zero and two zero voltage vectors of the inverter by taking into account the instantaneous discrepancies in torque and stator flux magnitude. The DTC induction motor drive presents a notable difficulty due to the presence of torque and flux ripples, which result from the incapability of any inverter switching vector to produce the exact stator voltage required for desired variations in torque and flux. As a result, a comprehensive examination of torque ripple becomes essential.

It is advisable to employ narrow flux hysteresis bands when using high-speed switching semiconductor devices. This is because the switching losses of these devices are typically minimal when compared to state losses. By implementing this approach, the hysteresis band can be adjusted to a sufficient size to restrict the inverter switching frequency below a specific threshold, typically determined by the thermal limitations of the power devices. Nevertheless, adjusting the hysteresis bands to accommodate extreme situations unavoidably leads to a decrease in the system's efficiency within a specific operational range, particularly in a region characterized by low speeds. The operating conditions can be used to modify the transition time from the lower to upper limit, and vice versa, in a torque hysteresis controller. The subsequent section introduces a fuzzy method to minimize torque ripple. Figure 5 depicts the model diagram of TS-Fuzzy based DTC for an induction motor. Additionally, a phase reconstruction module is included to obtain the three-phase voltage without the need for direct voltage measurement at the inverter output. This can help decrease the requirement for voltage sensors and ultimately lead to cost savings.

4. SVPWM Technique

Figure 6 provides the details on how to generate pulses using space vector pulse width modulation (SVPWM). It includes the trajectory of the space vector and the corresponding angle between vectors. The three phases, denoted as A, B, and C, each consist of two

switches positioned as upper and lower legs. By considering the angle, the SVPWM technique can effectively reduce harmonics in the inverter's output and enable quick motor control compared to other pulse generators. Unlike traditional methods that rely on a carrier waveform, SVPWM calculates the duty cycles of switches to synthesize the desired average output voltage. Additionally, SVPWM can generate a higher level of fundamental voltage compared to sinusoidal pulse width modulation, resulting in decreased total harmonic distortion (THD).

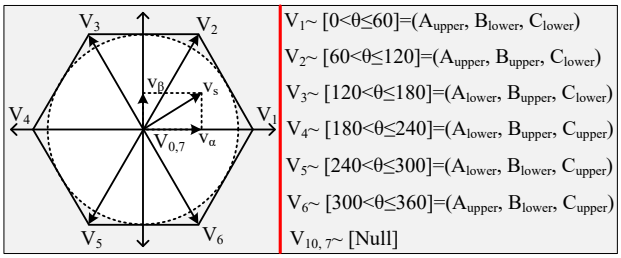

Fig. 6: SVPWM technique

5. Results

The MATLAB Simulink software is used to model the system depicted in Figure 1. Real-time simulators (RTSs) modules have the ability to efficiently solve power system equations, enabling them to effectively operate complex systems in real-time. This allows it to continuously generate output conditions that accurately represent the conditions in the actual network [1]. The RTS technology has gained widespread acceptance as an excellent tool for designing, developing, and testing of various power system control schemes. In order to implement the Hardware-in-the-Loop (HIL) setup, researchers have utilized two RTS modules developed by OPAL-RT technologies. Unit-1 accommodates the entire plant model, whereas unit-2 accommodates the suggested control approach. Both units are equipped with analog and digital cards to make a loop by interconnecting them. The control unit will receive the analog signals from the plant, while digital signals are sent from the control to the plant. Extensive results are extracted through another computer for the examination of results under various operating conditions. Figure 7 illustrates the HIL configuration established using two OPAL RT-OP5700 modules. Furthermore, the outcomes are presented in the subsequent case studies.

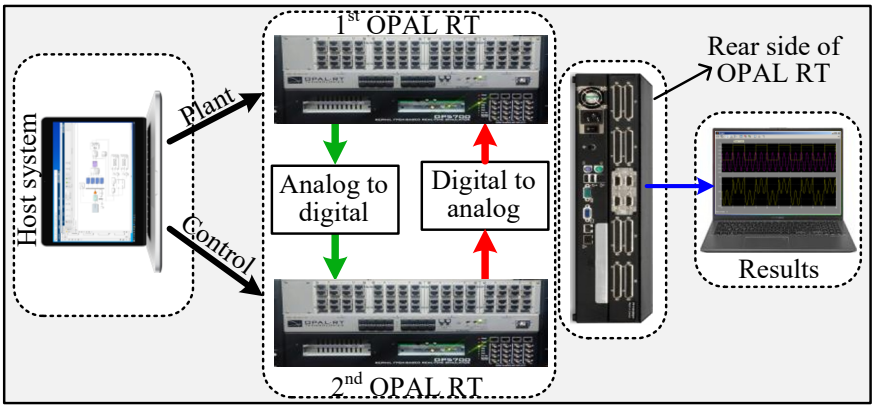

Fig. 7: HIL architecture.

Case-A: operation with motor

All aquaculture facilities require the implementation of variable speed controls to manage oxygen in fish ponds. Likewise, variable speed controls are essential for regulating the flow of water in various industries and residential buildings. As a result, the system's performance is evaluated when there is a change in the speed reference signal. At t=1.0 sec, the reference speed is adjusted from 900rpm to 1400rpm. The TS-fuzzy based DTC system generates the necessary pulses for the inverter to track the motor's reference speed. The comparison between the reference speed and the actual speed of the motor is presented in Figure 8. The flux components on the direct and quadrature axes are illustrated in Figure 9, showing a smooth profile that indicates the motor's smooth operation. The total flux is displayed in Figure 10, with the reference flux set to unity, resulting in a stable total flux at a unit value. This demonstrates that the motor is functioning safely in both saturation and flux weakening modes. The corresponding torque is shown in Fig. 11, while the AC and DC-link voltages are depicted in Fig. 12 (a) and (b) respectively.

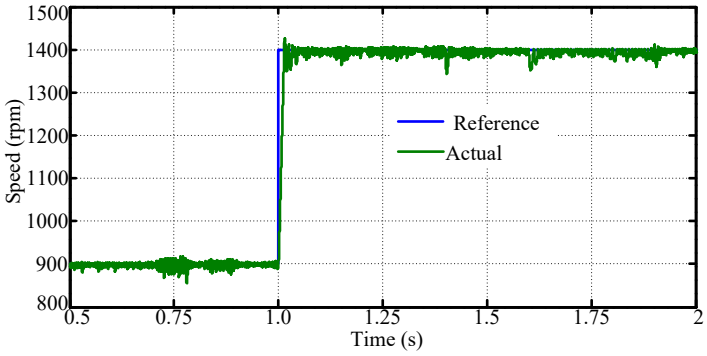

Fig. 8: Speed response.

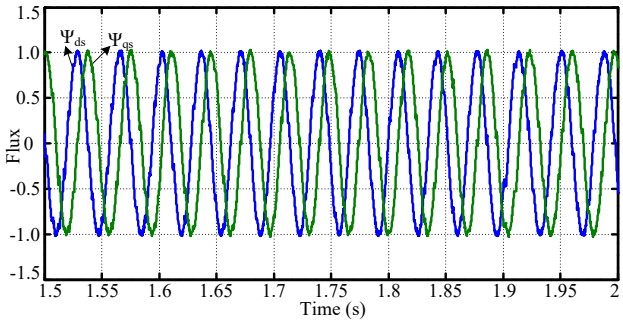

Fig. 9: Flux components.

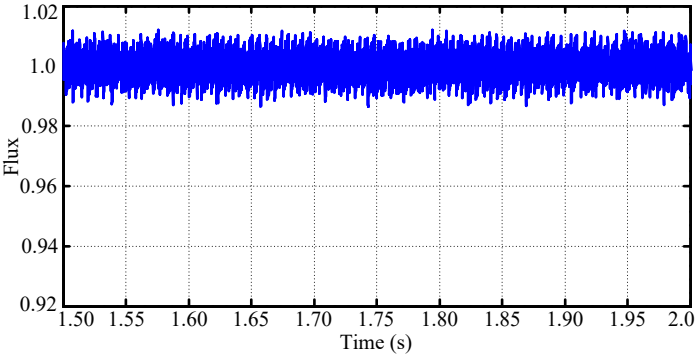

Fig. 10: Flux of motor.

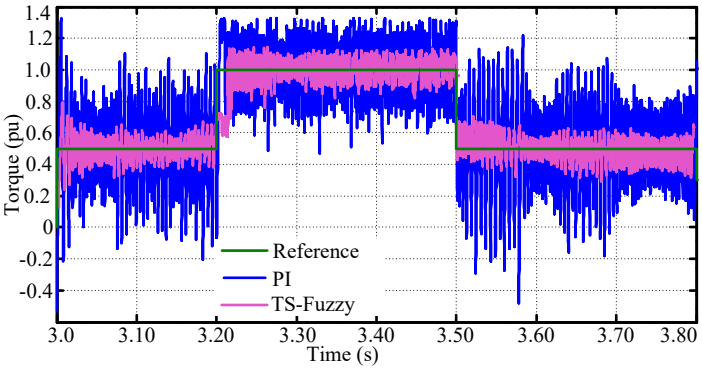

Fig. 11: Torque in per unit (pu).

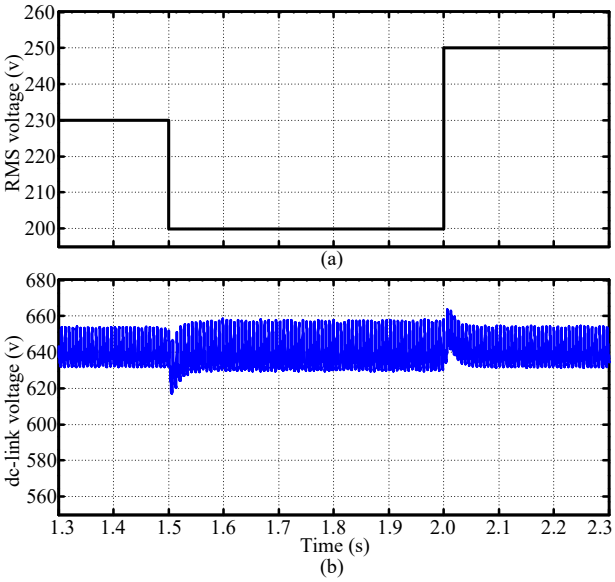

Fig. 12: Response of (a) single phase rms voltage, (b) dc-link voltage.

Case-B: operation without motor

In case of no operation with motor, the power generated from renewable sources should feed into battery and grid. The operation without operating motor drive is depicted in Fig. 13. Once, battery is fully charged, the grid can observe the power generated through sources.

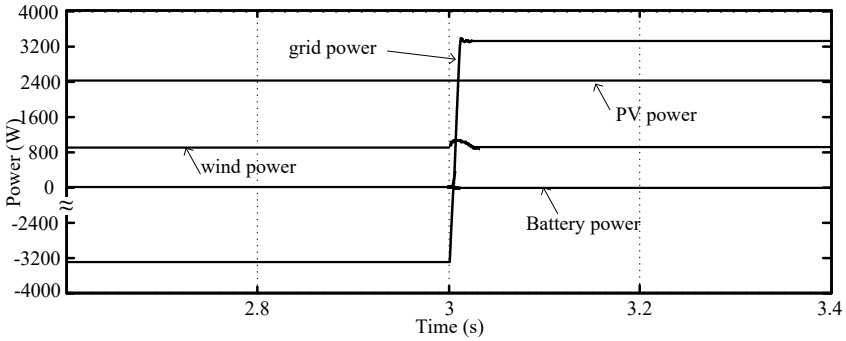

Fig. 13: Response of various powers.

6. Conclusion

The water pumping system, driven by a single-phase supply and a three-phase induction motor, has been equipped with TS-Fuzzy and sliding mode based controllers. In this paper, a sensorless controller has been proposed specifically for submersible pumps. The experimental results demonstrate the performance of the system under varying torque and reference speed conditions for different applications. Furthermore, an evaluation has been carried out to compare the electromagnetic torque produced by the motor when utilizing a PI controller versus a TS-Fuzzy controller. The evaluation reveals a significant advantage in favor of the TS-Fuzzy controller, as it effectively minimizes torque ripples in the DTC of the induction motor. To further enhance the system's efficiency, the integration of PV, wind, and battery bank technologies has been implemented to reduce diesel consumption. Furthermore, the extra power generated by the system can be transmitted to the grid in cases where the load power is less than the generation capacity, due to the controllers that have been recommended.

References:

[1] B. G. Fernandes et al, "A Single-Stage Sensorless Control of a PV-Based Bore-Well Submersible BLDC Motor", *IEEE Journal of Emerging and Selected Topics in Power Electronics*, Volume: 7, Issue: 2, June 2019

[2] C. N. Bhende, S. G. Malla, "Novel Control of Photovoltaic based Water Pumping System without Energy Storage", *International Journal of Emerging Electric Power Systems,* vol. 13, no. 4, 2012.

[3] S. Sashidhar, B. G. Fernandes, "A Novel Ferrite SMDS Spoke-Type BLDC Motor for PV Bore-Well Submersible Water Pumps," *IEEE Transactions on Industrial Electronics*, vol. 64, no. 1, pp. 104-114, 2017.

[4] R. Kumar, B. Singh, "Single Stage Solar PV Fed Brushless DC Motor Driven Water Pump," *IEEE Journal of Emerging and Selected Topics in Power Electronics*, vol. 5, no. 3, pp. 1377-1385, 2017.

[5] K. K. Prabhakaran, A. Karthikeyan, S. Varsha, B. V. Perumal, S. Mishra, "Standalone Single Stage PV-Fed Reduced Switch Inverter Based PMSM for Water Pumping Application," *IEEE Transactions on Industry Applications*, vol. 56, no. 6, pp. 6526-6535, 2020.

[6] M. N. Ibrahim, H. Rezk, M. Al-Dhaifallah, P. Sergeant, "Solar Array Fed Synchronous Reluctance Motor Driven Water Pump: An Improved Performance Under Partial Shading Conditions," *IEEE Access*, vol. 7, pp. 77100-77115, 2019.
[7] S. Shukla, B. Singh, "Reduced-Sensor-Based PV Array-Fed Direct Torque Control Induction Motor Drive for Water Pumping," *IEEE Transactions on Power Electronics*, vol. 34, no. 6, pp. 5400-5415, 2019.
[8] M. J. M. Rao, M. K. Sahu, P. K. Subudhi, "PV based water pumping system for agricultural sector," *Materials Today: Proceedings*, vol. 5, no. 1, 1008-1016, 2018.
[9] A. Betka, A. Moussi, "Performance Optimization of a Photovoltaic Induction Motor Pumping System", *Renewable Energy*, vol. 29, no. 14, pp. 2167-2181, 2004, doi: 10.1016/j.renene.2004.03.016.
[10] M. Arrouf, N. Bouguechal, "Vector control of an Induction Motor fed by a Photovoltaic Generator", *Applied Energy*, vol. 74, no. 1-2, pp. 159-167, 2003, doi: 10.1016/S0306-2619(02)00142-3.
[11] J. R. Arribas, C. M. V. González, "Optimal Vector Control of Pumping and Ventilation Induction Motor Drives", *IEEE Transactions on Industrial Electronics*, vol. 49, no. 4, pp. 889-895, 2002, doi: 10.1109/TIE.2002.801240.
[12] M. A. Elgendy, B. Zahawi, D. J. Atkinson, "Comparison of Directly Connected and Constant Voltage Controlled Photovoltaic Pumping Systems", *IEEE Transactions on Sustainable Energy*, vol. 1, no. 3, pp. 184-192, 2010, doi: 10.1109/TSTE.2010.2052936.
[13] http://www.irrigationtutorials.com/pump.htm
[14] C. N. Bhende, S. Mishra, S. K. Jain, "TS-fuzzy-controlled active power filter for load compensation", *IEEE Transactions on Power Delivery,* vol. 21, no. 3, pp. 1459-1465, 2006, doi: 10.1109/TPWRD.2005.860263.
[15] B. K. Bose, "*Modern Power Electronics and AC Drives"*, PHI Learning, 2010.
[16] C. C. Chan, W. S. Leung, C. W. Ng, "Adaptive Decoupling Control of Induction Motor Drives", *IEEE Transactions on Industrial Electronics*, Vol. 37, No. 1, pp. 41-47, 1990, doi: 10.1109/41.45842.
[17] A. M. Khambadkone, J. Holtz, "Vector-Controlled Induction Motor Drive with a Self-Commissioning Scheme", *IEEE Transactions on Industrial Electronics*, vol. 38, no. 5, pp. 322-327, 1991, doi: 10.1109/41.97551.
[18] G. O. Garcia, J. C. Mendes Luis, R. M. Stephan, E. H. Watanabe, "An Efficient Controller for an Adjustable Speed Induction Motor Drive", *IEEE Transactions on Industrial Electronics*, vol. 41, no. 5, pp. 533-539,1994, doi: 10.1109/41.315272.
[19] A. K. Abdelsalam, M. I. Masoud, M. S. Hamad, B. W. Williams, "Modified Indirect Vector Control Technique for Current-Source Induction Motor Drive", *IEEE Transactions on Industry Applications*, vol. 48, no. 6, pp. 2433-2442, 2012, doi: 10.1109/TIA.2012.2227132.
[20] J, Guzinski, H. Abu-Rub, "Speed Sensorless Induction Motor Drive with Predictive Current Controller", *IEEE Transactions on Industrial Electronics*, Vol. 60, No. 2, pp. 699-709, 2013, doi: 10.1109/TIE.2012.2205359.
[21] Z. Yan, C. Jin, V. I. Utkin, "Sensorless Sliding-Mode Control of Induction Motors", *IEEE Transactions on Industrial Electronics*, vol. 47, no. 6, pp. 1286-1297, 2000, doi: 10.1109/41.887957.
[22] M. Bhardwaj,"Sensorless Field Oriented Control of 3-Phase Induction Motors Using F2833x", *Application Report*, Texas Instruments Incorporated, 2013.
[23] K. S. Jairaj, K. Srikant, "Simulation and Testing of Induction Motors Used with Irrigation Pumps", *International Journal of Automation and Power Engineering*, vol. 1, no. 2, pp. 23-28, 2012.
[24] D. Ismail, A. Karem, M. Irwanto, N. Gomesh, M. Muzhar, M. Asri, "Parameters calculation of 5 HP AC induction motor" in *International Conference on Applications and Design in Mechanical Engineering (ICADME),* Batu Ferringhi, Penang, Malaysia, 2009.
[25] http://www.kirloskarpumps.com/download/prod_catalogue/Motor%20Catalogue.pdf